Data in Brief 31 (2020) 106015

Contents lists available at ScienceDirect

Data in Brief

journal homepage: www.elsevier.com/locate/dib

Data Article

Petrographic and mineral-glass chemical dataset of igneous rock clasts from Early Oligocene Aveto-Petrignacola Formation (Northern Italy)

Michele Mattioli[a,*], Michele Lustrino[b,c], Sara Ronca[b], Gianluca Bianchini[d]

[a] Dipartimento di Scienze Pure e Applicate, Università di Urbino Carlo Bo, Campus Scientifico Mattei, 61029 Urbino, Italy
[b] Dipartimento di Scienze della Terra, Università degli Studi di Roma La Sapienza, P.le A. Moro, 5, 00185 Roma, Italy
[c] Istituto di Geologia Ambientale e Geoingegneria (IGAG) CNR, c/o Dipartimento di Scienze della Terra, Università degli Studi di Roma La Sapienza, P.le A. Moro, 5, 00185 Roma, Italy
[d] Dipartimento di Fisica e Scienze della Terra, Università degli Studi di Ferrara, Via Saragat, 1, 44100 Ferrara, Italy

ARTICLE INFO

Article history:
Received 16 June 2020
Revised 5 July 2020
Accepted 7 July 2020
Available online 12 July 2020

Keywords:
Aveto-Petrignacola Formation
Canetolo Unit
Calc-alkaline magmatism
Volcaniclastic succession
Northern Apennines

ABSTRACT

This dataset article contains petrographic and mineral-glass chemical data of igneous rock clasts from Early Oligocene Aveto-Petrignacola Formation (APF; Northern Italy). Methods for obtaining the dataset include optical microscopy, scanning electron microscopy and electron probe microanalysis. The APF volcanic rocks are basalts, basaltic andesites, andesites, dacites and rhyolites. Rare gabbroic cumulate nodules complete the dataset. Basalts are porphyritic, with calcic plagioclase ($An_{72-92}Ab_{7-27}Or_{0-1}$), ferroan enstatite ($En_{59-68}Fs_{29-37}Wo_{3-4}$) and augite ($En_{38-39}Fs_{18-20}Wo_{41-44}$) phenocrysts, in a hypocrystalline groundmass made up of bytownite ($An_{71-85}Ab_{14-28}Or_1$), augite ($En_{37-38}Fs_{19}Wo_{43-44}$), ferroan enstatite ($En_{62-68}Fs_{30-35}Wo_{1-4}$) and rare pigeonite ($En_{46-50}Fs_{37-42}Wo_{7-17}$). The basaltic andesites are porphyritic to glomeroporphyritic with phenocrysts of zoned plagioclase ($An_{44-67}Ab_{32-55}Or_1$), orthopyroxene, Mg-rich augite

DOI of original article: 10.1016/j.lithos.2011.12.017
* Corresponding author.
E-mail address: michele.mattioli@uniurb.it (M. Mattioli).

https://doi.org/10.1016/j.dib.2020.106015

($En_{38-42}Fs_{15-17}Wo_{43-45}$), rare pargasite to edenite amphibole (Mg# 69–59) and very rare biotite in a hypocrystalline to holohyaline groundmass. Andesites are highly porphyritic with phenocrysts of plagioclase ($An_{47-79}Ab_{20-52}Or_{0-1}$), pargasite to magnesio-hornblende (Mg# 72–67), Mg-rich augite ($En_{43-46}Fs_{12-17}Wo_{41-43}$), subordinate ferroan enstatite ($En_{68-74}Fs_{23-29}Wo_{3-4}$), biotite (Mg# 53) and Ti-magnetite (Usp_{29-41}). Dacites (massive lavas and ignimbrites) are porphyritic, with phenocrysts and phenoclasts of plagioclase ($An_{33-79}Ab_{20-62}Or_{0-4}$), calcic amphibole (Ti-pargasite, Mg-hornblende and edenite; Mg# 81–46), biotite (Mg# 67–56), very rare Mg-rich augite ($En_{41-42}Fs_{16-18}Wo_{40-43}$) and resorbed quartz in hypohyaline to holohyaline groundmass with a dense mat of anhedral quartz, labradorite-andesine ($An_{36-66}Ab_{33-61}Or_{1-4}$) and rare anorthoclase ($An_{22}Ab_{66}Or_{12}$). Rhyolitic compositions have been found both as volcanic clasts (massive lava and ignimbrites) with andesine to oligoclase phenoclasts ($An_{25-38}Ab_{61-71}Or_{1-4}$), quartz, biotite (Mg# 55–53) and Ti-magnetite (Usp_{18-77}), and as interstitial glasses (residual melt drops) in other APF volcanic rocks. The cumulate nodules are olivine-gabbro and amphibole-gabbro/gabbronorite with a mineral paragenesis dominated by plagioclase ($An_{41-73}Ab_{26-57}Or_{1-3}$), olivine ($Fo_{68-72}$), Mg-rich augite to ferroan diopside ($En_{41-45}Fs_{12-15}Wo_{42-45}$; Mg# 79–74), ferroan enstatite ($En_{65-74}Fs_{24-33}Wo_{2-3}$; Mg# 76–68), magnetite (Usp_{15-28}) and titanian pargasite (Mg# 67–65). The main cumulus phases are plagioclase, olivine and pyroxene, while intercumulus/postcumulus phases are titanian pargasite and magnetite. The dataset can be used to compare petrographic features and chemical compositions of calc-alkaline rocks emplaced in other subduction-related settings. Above all, it can represent a useful contribution in solving the problem linked to the identification of a hidden Early-Oligocene source of the thick volcaniclastic APF succession in the Alpine-Apennine belt geodynamic evolution.

Specifications Table

Subject	Earth and Planetary Sciences
Specific subject area	Geology, mineralogy, petrography
Type of data	Tables, images, graphics
How data were acquired	Optical polarizing microscope: Nikon Optiphot2-Pol, equipped with AxioScope Digital Camera. Environmental Scanning Electron Microscopes (ESEM): FEI Quanta 200 FEG, equipped with an energy-dispersive X-ray spectrometer (EDS) for microchemical analyses. Electron Micro Probe (EMP): four wavelength dispersion spectrometers Cameca SX50 and Camebax Microbeam 799.
Data format	Raw, analyzed

(*continued on next page*)

Parameters for data collection	About 300 samples of igneous rock clasts were collected in the field, fifty-nine of which (very fresh samples) were selected and analysed. Representative polished thin sections were mounted in aluminum stub for ESEM observations and analysis; operating conditions were a 30 kV accelerating potential, 2–15 nA beam current, 10 mm working distance, 0° tilt angle, variable beam diameter, low vacuum mode, with a specimen chamber pressure set from 0.80 to 0.90 mbar. The same polished thin sections were metallized for EMP analysis performed with an electronic beam diameter of 5–7 μm, an acceleration voltage of 15 kV and a beam current of 10 nA. The electron beam was defocused, with a shortened accumulation time (from 100 s down to 50 s) to minimizes volatile migration and loss. The standards used were natural minerals and synthetic phases.
Description of data collection	Modal mineralogy and petrography were identified in thin section using an optical polarizing microscope. Scanning Electron Microscopy (SEM) and Energy Dispersion Spectroscopy (EDS) was used to verify the semi-quantitative elemental composition of mineral phases and glass. Chemical composition of selected mineral phases and glass was finally determined using wavelength dispersive spectroscopy on EMP.
Data source location	Val d'Aveto, 44° 36′ 51″ N, 9° 23′ 57″ E Petrignacola, 44° 30′ 32″ N, 10° 07′ 04″ E Campastrino, 44° 22′ 47″ N, 10° 17′ 37″ E
Data accessibility	With the article
Related Research Article	M. Mattioli, M. Lustrino, S. Ronca, G. Bianchini, Alpine subduction imprint in Apennine volcaniclastic rocks. Geochemical-petrographic constraints and geodynamic implications from Early Oligocene Aveto-Petrignacola Formation (N Italy), Lithos 134–135 (2012) 201–220 [4]. doi:10.1016/j.lithos.2011.12.017

Value of the Data

- Petrography, mineral phases and glass from igneous rock clasts of Aveto-Petrignacola Formation, Northern Apennines, have been described and chemically characterized for both local and regional comparisons: this is the only dataset containing chemical data for these igneous rocks.
- The data presented here may be used by other authors to compare petrographic features and chemical compositions of similar calc-alkaline igneous rocks discovered in worldwide collisional zones.
- The characterization of these rocks could be a useful contribution in solving the problem linked to the hidden Early-Oligocene magmatism in the geodynamic evolution of the Alps-Apennine thrust systems.
- The achieved dataset can be compared with those obtained from similar geologic environments and motivate studies on volcano-sedimentary sequences in the future.

1. Data Description

This data article contains petrographic and mineral-glass chemical data of igneous rock clasts from the Aveto-Petrignacola Formation, Northern Italy (Fig. 1) [1,2]. The Aveto-Petrignacola Formation (hereafter APF) is one of the most interesting clastic deposits of Italy, representing one of the few scattered remnants of the volcanic activity that developed during Tertiary time in the Northern Apennine [2–4]. Although a recent work has highlighted the geochemical characteristics and the origin of the APF volcanites [4], the Early Oligocene magmatism remains a puzzle in the geodynamic evolution of the Alps-Apennine fold-and-thrust systems [5–8]. In this dataset, igneous rock clasts of the APF are characterized by optical microscopy, scanning electron microscopy and electron probe microanalysis. Petrographic features are shown in mi-

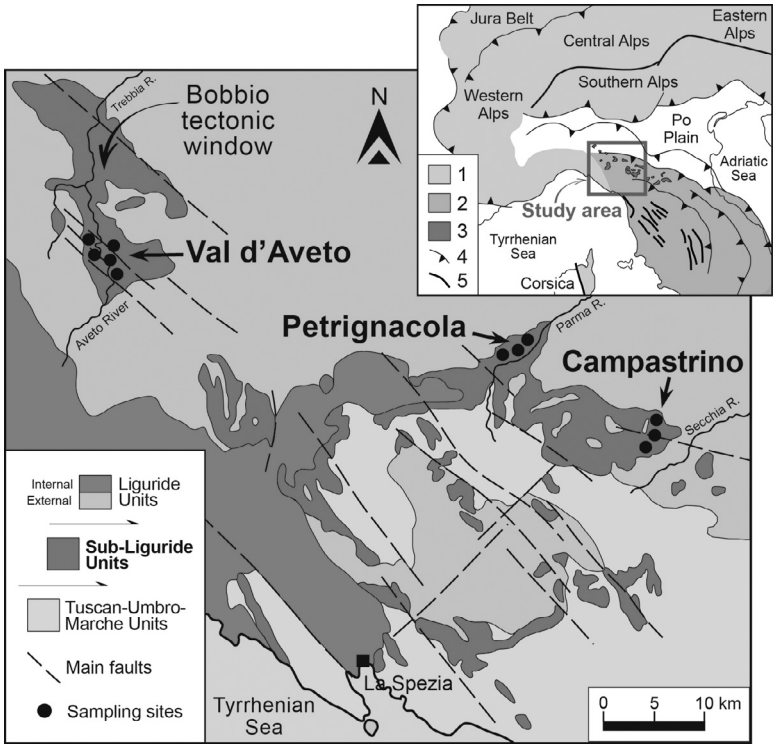

Fig. 1. Sketch map of the distribution of the Sub-Liguride Units (including Aveto-Petrignacola Formation) in the northern Apennines with indication of the sampling sites (modified from [2]). Legend: 1 = Alpine thrust belt units; 2 = Northern Apennines units; 3 = Sub-Liguride Units; 4 = thrusts; 5 = faults.

crophotographs of Figs. 2a and 2b, while chemical compositions of mineral phases and glass are reported in Tables 1, 2 (see Supplementary Tables 1–6) and illustrated in Figs. 3–6.

The APF basalts are porphyritic, locally glomeroporphyritic, often seriate, with PI (Porphyritic Index = area of phenocrysts over the total area of the thin section x 100) up to 25%. The phenocrysts consist of plagioclase, pyroxene and Fe-Ti oxides set in a hypocrystalline, rarely holohyaline, intersertal to pilotaxitic groundmass. The plagioclase phenocrysts are particularly Ca-rich ($An_{72-92}Ab_{7-27}Or_{0-1}$, form clear, euhedral crystals and are unzoned or slightly normally zoned, and groundmass grains are only slightly less calcic, with bytownitic composition ($An_{71-85}Ab_{14-28}Or_1$). Pyroxene phenocrysts are both ferroan enstatite ($En_{59-68}Fs_{29-37}Wo_{3-4}$; Mg# 61–70) and magnesium-rich augite ($En_{38-39}Fs_{18-20}Wo_{41-44}$; Mg# 70–71), whereas the groundmass pyroxenes are augite ($En_{37-38}Fs_{19}Wo_{43-44}$; Mg# 68–69), ferroan enstatite ($En_{62-69}Fs_{30-35}Wo_{1-4}$); Mg# 65–70) and rare pigeonite ($En_{46-50}Fs_{37-42}Wo_{7-17}$; Mg# 55–60). Fe-Ti oxides belong to the rhombohedral phase group (Ilm_{93-99}) and spinel group (Usp_{35-57}).

The APF basaltic andesites are porphyritic to glomeroporphyritic (PI ~30–40%) and resemble basalts in their mineralogy. Phenocrysts of plagioclase, orthopyroxene, clinopyroxene, opaques and very rare amphibole and biotite are set in a hypocrystalline to holohyaline groundmass. Plagioclase is zoned ($An_{44-67}Ab_{32-55}Or_1$) and exhibits various textures, including clear euhedral grains, subhedral crystals in glomeroporphyritic aggregates, but also occurs as sieved laths with complex zoning patterns. Clinopyroxene is magnesium-rich augite ($En_{38-42}Fs_{15-17}Wo_{43-45}$; Mg# 72–79), amphibole ranges from pargasite to edenite (Mg# = 59–69) and the main opaque minerals are Ti-magnetite (Usp_{16-45}) and ilmenite (Ilm_{92-94}). Early formed orthopyroxene crystals are often overgrown by an augitic clinopyroxene rim.

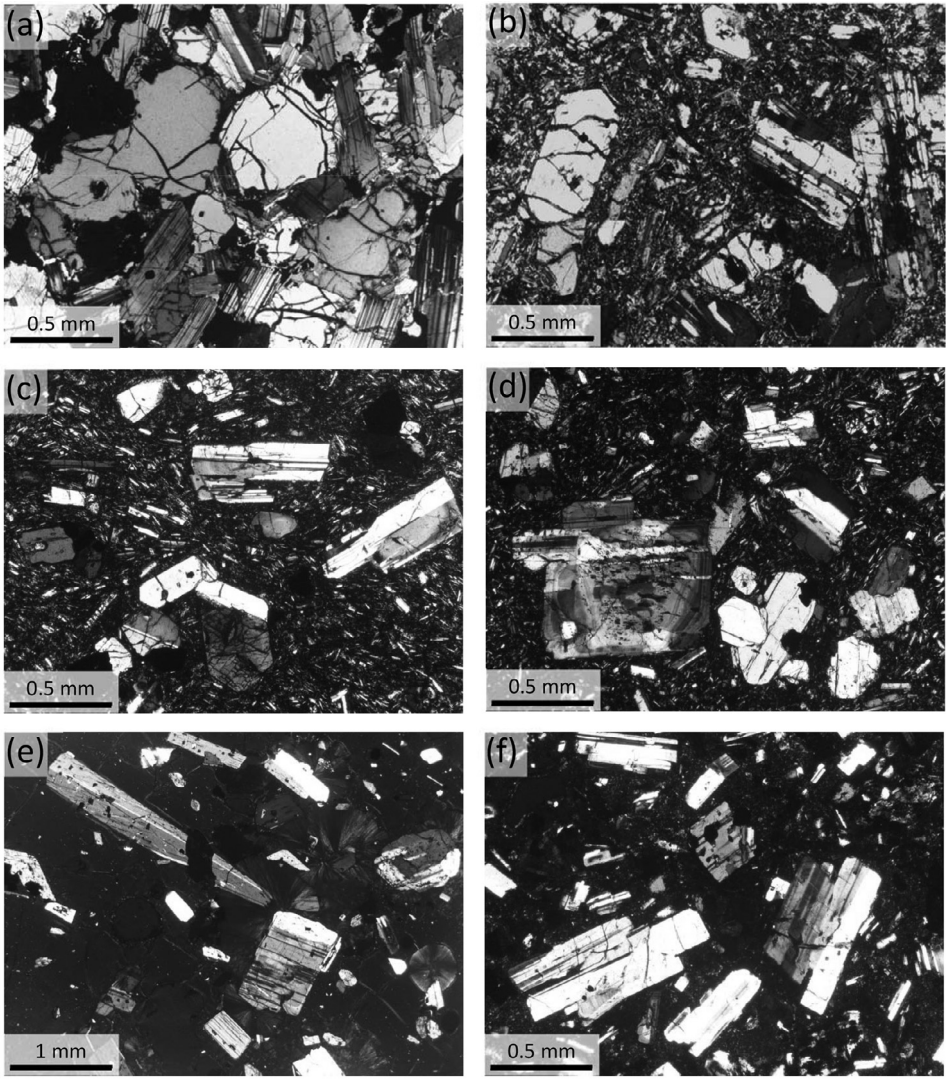

Fig. 2a. Crossed polarized light photomicrographs showing the typical textures of representative fresh samples of APF igneous rocks. (a) Olivine gabbro: plagioclase, magnetite, olivine and minor clinopyroxene with a cumulate texture (sample APF 405). (b) Basalt: plagioclase and orthopyroxene phenocrysts in a hypocrystalline groundmass (sample APF 120). (c) Basaltic andesite: plagioclase, clinopyroxene, orthopyroxene and Ti-magnetite phenocrysts in a hypocrystalline groundmass (sample APF 408). (d) Andesites: zoned plagioclase, clinopyroxene and orthopyroxene crystals in cryptocrystalline groundmass (sample APF 403). (e) Dacite: vitrophyric texture, with zoned plagioclase, twinned amphibole and biotite phenocrysts in a holohyaline, partially perlitic groundmass with a spherulitic texture (sample APF 409). (f) Rhyolite: amphibole and plagioclase phenocrysts in a hypocrystalline groundmass (sample APF 407).

The APF andesites are porphyritic (PI ~20–50%), with phenocrysts of plagioclase, amphibole, clinopyroxene, subordinate orthopyroxene, rare biotite and Fe-Ti oxides. The groundmass is hypocrystalline to holohyaline and consists of fine, anhedral patches of feldspar, two pyroxenes and cryptocrystalline material. Plagioclase phenocrysts are less calcic than those in basalts and basaltic andesites ($An_{47-79}Ab_{20-52}Or_{0-1}$) and can be clumped, broken, rounded or euhedral, equant to slightly elongated. Very elongated plagioclase laths are found in the groundmass only,

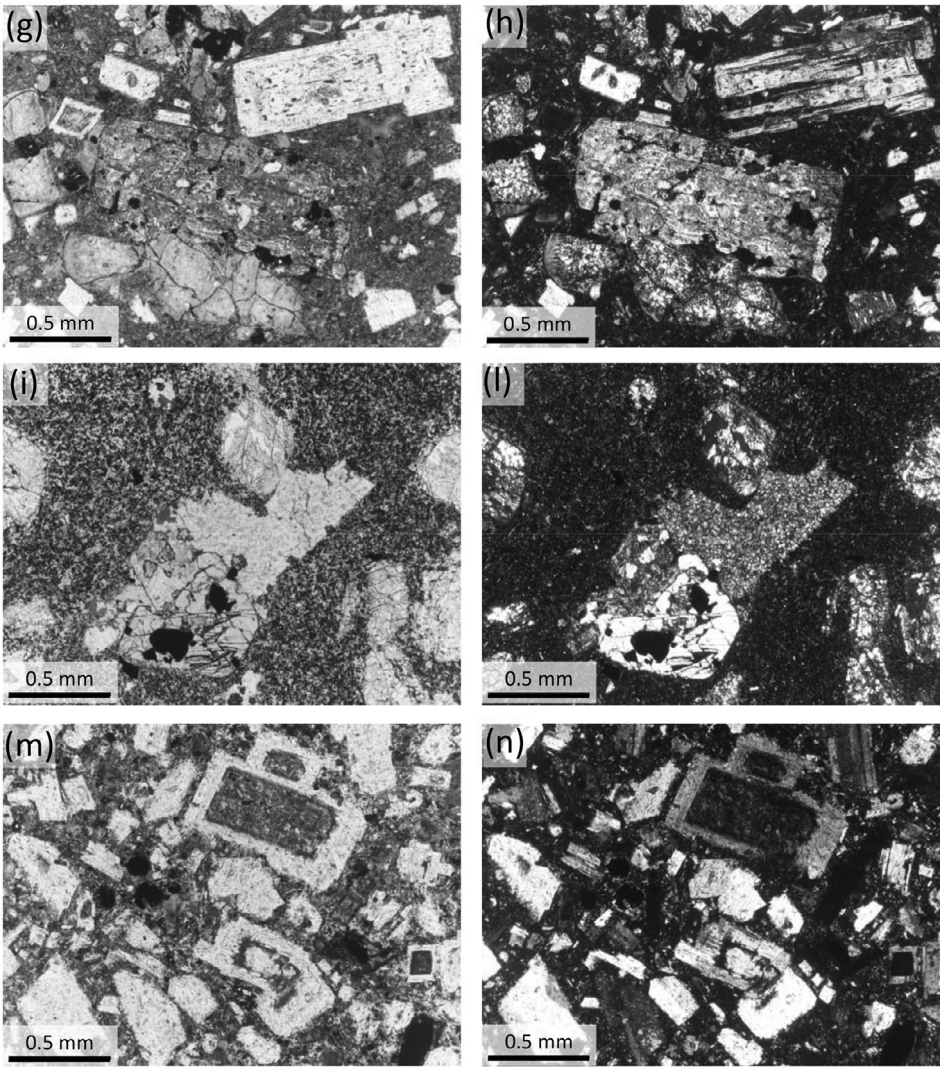

Fig. 2b. Photomicrographs of slightly altered samples of APF igneous rocks. These samples have not been used for mineral and glass chemical analyses, but they are showed only for comparison purposes. (g,h) basalt: plagioclase and altered mafic minerals in a hypocrystalline groundmass (g = plane polarized light, h = cross polarized light; sample APF 15b). (i,l) Basaltic andesite: sericitized plagioclase, opaques and mafic phenocrysts in a cryptocrystalline groundmass (i = plane polarized light, l = cross polarized light; sample APF 2b). (m,n) andesite: partially altered plagioclase, mafic and opaques phenocrysts in a hypocrystalline groundmass (m = plane polarized light, n = cross polarized light; sample APF 14a).

where it shows a labradoritic composition ($An_{53-61}Ab_{38-46}Or_{1-2}$). Variable disequilibrium with host melt(s) is represented by spongy zones in the core, on the rim, or in between. Spongy cores may be either more or less anorthitic than surrounding clear rims. Plagioclase generally exhibits oscillatory and reverse zoning. Clinopyroxene is a magnesium-rich augite ($En_{43-46}Fs_{12-17}Wo_{41-43}$; Mg# 77–81), with phenocrysts stubby to equant habit, euhedral to subhedral shape, showing only slight zoning. Groundmass augite is more Si-rich and Ti-poor than phenocrysts. Orthopyroxene is ferroan enstatite ($En_{68-74}Fs_{23-29}Wo_{3-4}$; Mg# 70–77) showing a slight Ca increase in the groundmass crystals. Amphibole ranges in composition from pargasite to magnesio-hornblende

Table 1
Chemical compositions of olivine of the APF igneous rock. Abbreviations: GA = gabbro; corr = corroded crystal; cum = cumulus phase; intergr = intergranular.

Sample	APF405	APF405	APF405	APF405	APF405	APF405
Rock type	GA	GA	GA	GA	GA	GA
Comment	corr	cum	cum	cum	cum	intergr
SiO_2	38.43	37.89	38.22	38.14	37.76	38.15
MgO	36.75	34.07	33.62	33.64	34.71	34.62
CaO	0.05	0.05	0.06	0.05	0.07	0.04
Cr_2O_3	0.07	0.10	0.07	0.03	0.07	0.01
MnO	0.65	0.81	0.76	0.75	0.73	0.64
FeO_{tot}	24.98	28.70	28.22	27.37	26.28	27.25
NiO	–	–	–	–	0.03	0.07
Sum	100.96	101.63	100.95	100.01	99.65	100.80
Si	1.00	1.00	1.01	1.02	1.01	1.01
Fe^{2+}	0.55	0.63	0.63	0.61	0.59	0.60
Mn	0.01	0.02	0.02	0.02	0.02	0.01
Mg	1.43	1.34	1.33	1.34	1.38	1.36
Ca	0.00	0.00	0.00	0.00	0.00	0.00
Cr	0.00	0.00	0.00	0.00	0.00	–
Ni	–	–	–	–	0.00	0.00
Sum	2.99	3.00	2.99	2.98	2.99	2.99
Fo	72.39	67.91	67.99	68.66	70.19	69.37
Fa	27.61	32.09	32.02	31.34	29.81	30.63

(Mg# 67–72) and is rimmed by, or sometimes partly converted to, fine-grained aggregates of opaque minerals. Biotite is rare (Mg# ~53) and is often partially or completely transformed to chlorite and/or opaque minerals. Fe-Ti oxides are Ti-magnetite (Usp_{29-41}) occurring as microphenocrysts and as inclusions in pyroxenes.

The APF dacites have PI ranging from ~20 to ~40% with phenocrysts (phenoclasts in the ignimbrite facies) of plagioclase ($An_{33-79}Ab_{20-62}Or_{0-4}$), calcic amphibole (titanian pargasite, magnesio-hornblende and edenite, Mg# 46–81), biotite (Mg# 56–67), very rare Mg-rich augite ($En_{41-42}Fs_{16-18}Wo_{40-43}$; Mg# 71–72) and resorbed quartz; ferroan enstatite ($En_{66-68}Fs_{29-32}Wo_{3-4}$; Mg# ~70) occurs as phenocrysts in some trachytic types. Groundmass is hypohyaline to holohyaline, maily consisting of anhedral quartz, labradorite to andesine plagioclase ($An_{36-66}Ab_{33-61}Or_{1-4}$) and rare anorthoclase ($An_{22}Ab_{66}Or_{12}$), occasionally with microspherulitic textures. Ti-magnetite (Usp_{10-29}) and ilmenite$_{ss}$ (Ilm_{67-95}) occur as inclusions in mafic phenocrysts and in the groundmass. Dacitic ignimbrites are characterised by the predominance of vesiculated juvenile material, indicating a pyroclastic flow origin.

The most evolved APF rocks are massive lava and ignimbrites with ~30–40 vol.% andesine to oligoclase phenocrysts and phenoclasts ($An_{25-38}Ab_{61-72}Or_{1-4}$), quartz, biotite (Mg# 53–55), and Ti-magnetite (Usp_{18-77}). Ignimbrites generally show eutaxitic textures, with phenoclasts and lithic fragments embedded in a tuffaceous to devitrified groundmass. Pseudo-fluidal patterns are given by iso-oriented biotites and ribbons of opaque microcrystals. Several rhyolitic compositions have been also found as interstitial glasses (residual melt drops) in basalts, basaltic andesites and dacites (Fig. 6).

The APF volcanic clasts contain medium- to coarse-grained holocrystalline nodules, a feature which is common within calc-alkaline associations [9,10]. Most of the APF nodules display a cumulate texture and are classified as olivine-gabbro and amphibole-gabbro/gabbronorite. The mineral paragenesis is dominated by subhedral to euhedral plagioclase (45–70 vol.%, $An_{41-73}Ab_{26-57}Or_{1-3}$), subhedral to anhedral olivine (2–20 vol.%, Fo_{68-72}), subhedral Mg-rich augite to ferroan diopside clinopyroxene (5–15 vol.%, $En_{41-45}Fs_{12-15}Wo_{42-45}$; Mg# 74–79), subhedral ferroan enstatite (2–6 vol.%, $En_{65-74}Fs_{24-33}Wo_{2-3}$; Mg# 68–76), subhedral to euhedral magnetite (5–15 vol.%) and subhedral titanian pargasite (5–15 vol.%, Mg# 65–67). The main cumulus

Table 2
Chemical compositions of glass of the APF igneous rock. Abbreviations: R = rhyolite.

Sample Label	APF409	APF409	APF409	APF409	APF409	APF409	APF409	APF411	APF411	APF411	APF411	APF411	APF411	APF120	APF120	APF120	APF120	APF106	APF106	APF106	APF106
Rock Type	R	R	R	R	R	R	R	R	R	R	R	R	R	R	R	R	R	R	R	R	R
SiO_2	77.84	77.46	77.28	80.17	79.76	78.12	77.66	80.12	79.07	79.00	77.81	78.44	78.13	75.51	75.88	75.72	74.74	74.91	75.02	74.44	75.21
TiO_2	0.09	0.13	0.10	0.11	0.07	0.11	0.14	0.16	0.17	0.16	0.26	0.19	0.17	0.13	0.15	0.16	0.26	0.21	0.24	0.25	0.21
Al_2O_3	12.14	12.40	12.03	11.53	11.68	12.21	12.05	10.13	11.83	11.46	11.22	11.45	12.03	12.91	12.82	12.72	13.28	13.08	13.07	13.21	13.14
$Fe_2O_{3(tot)}$	0.78	0.82	0.71	0.41	0.47	0.70	0.70	0.75	0.88	0.89	1.09	0.75	0.92	1.15	1.04	1.23	1.44	1.36	1.51	1.54	1.34
MnO	0.02	0.04	0.03	0.07	0.05	0.06	0.00	0.03	0.06	0.04	0.06	0.02	0.06	0.04	0.02	0.02	0.05	0.04	0.02	0.06	0.03
MgO	0.08	0.10	0.08	0.00	0.06	0.09	0.06	0.12	0.10	0.08	0.28	0.04	0.06	0.03	0.04	0.04	0.06	0.06	0.05	0.07	0.04
CaO	0.84	0.88	0.92	0.92	0.91	0.65	0.88	0.63	0.56	0.52	0.43	0.55	0.65	1.69	1.02	1.41	2.03	2.24	2.11	2.27	2.21
Na_2O	2.14	2.35	2.33	4.28	3.50	2.34	2.17	1.57	2.60	2.59	2.30	2.58	2.77	2.98	3.01	3.22	3.54	3.44	4.91	4.89	3.57
K_2O	5.71	5.80	5.59	2.87	3.85	5.82	5.85	4.50	5.14	5.33	5.10	5.12	5.22	5.22	5.34	5.41	5.01	3.99	4.21	4.03	5.18
Sum	99.64	99.98	99.07	100.35	100.35	100.09	99.51	98.01	100.40	100.07	98.56	99.14	100.02	99.66	99.31	99.93	100.41	99.33	101.14	100.76	100.94

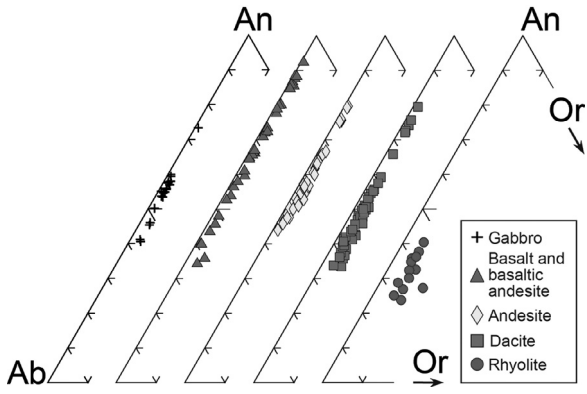

Fig. 3. Albite (Ab) - anorthite (An) - orthoclase (Or) ternary diagram for feldspars of the APF igneous rocks (modified from [4]).

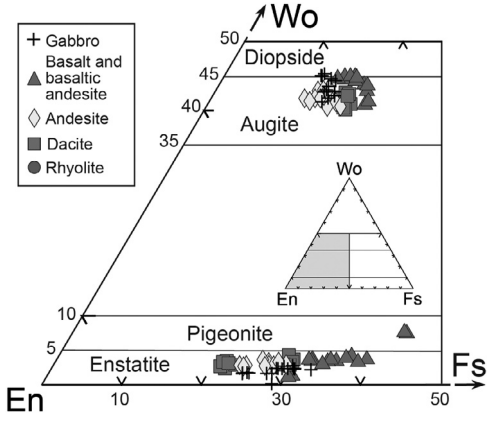

Fig. 4. Wollastonite (Wo) - enstatite (En) - ferrosilite (Fs) classification diagram for pyroxenes (after [10]) of the APF igneous rocks (modified from [4]).

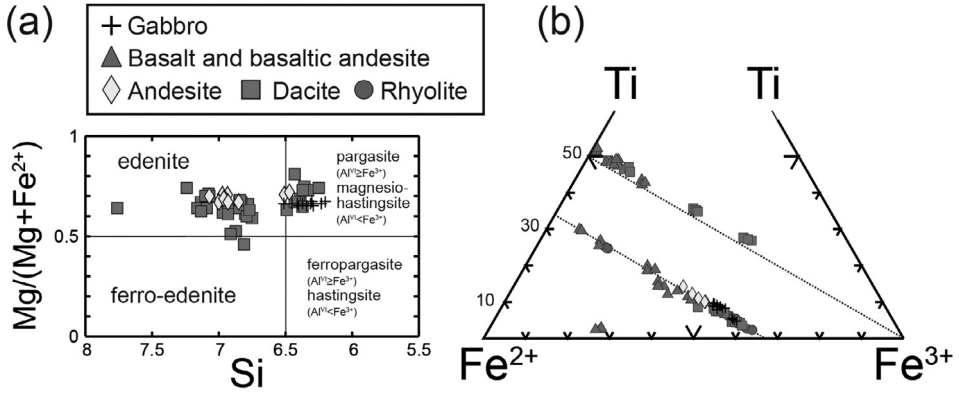

Fig. 5. (a) $Mg/(Mg+Fe^{2+})$ versus Si classification diagram for amphiboles (after [10]) and (b) $Ti\text{-}Fe^{2+}\text{-}Fe^{3+}$ ternary diagram for Fe-Ti oxides of the APF igneous rocks (modified from [4]).

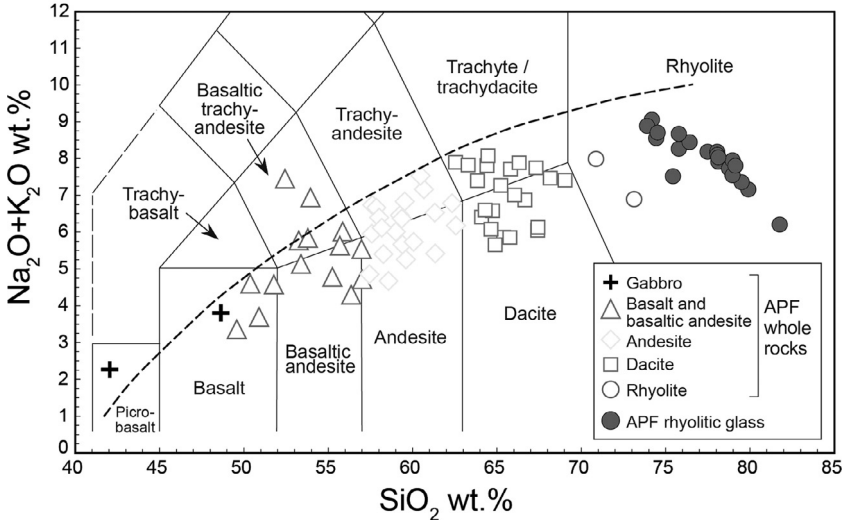

Fig. 6. Total alkali versus silica (TAS) diagram for the interstitial glasses of the APF volcanic rocks. Whole rock compositions of the APF igneous rocks (from [4]) are reported for comparison. Dashed line: alkaline-sub-alkaline division according to [17].

phase is plagioclase together with olivine and minor clinopyroxene in the olivine-gabbro, while clinopyroxene and orthopyroxene are the main cumulus minerals in the amphibole gabbronorite. Intercumulus/postcumulus phases are titanian pargasite and magnetite (Usp_{15-28}). Plagioclase generally forms elongate and euhedral laths up to 5 mm in length, olivine is typically resorbed and surrounded by symplectite coronas of pyroxene and magnetite. The other mafic phases are present as smaller (~0.5–1 mm large), anhedral to subhedral crystals. Pyroxene crystals often show reaction rims with amphibole, and apatite is the main accessory phase.

2. Experimental design, materials, and methods

2.1. Study area description

The Early Oligocene APF crops out discontinuously for ~200 km^2 along the northern Apennine belt (Fig. 1) and consists of a volcano-sedimentary sequence, whose thickness varies from ~150 m in the Parma and Secchia Valleys to ~1500 m in the Aveto Valley [1,2]. Lithic fragments of volcanic origin are dominant (65–80 vol.%), whereas other lithologies (plutonic, metamorphic and sedimentary rocks) are subordinate and essentially derived from the erosion of a basement and a sedimentary cover [2]. A large number of volcanic samples (~300) were collected from three key stratigraphic sections (Val d'Aveto, Petrignacola and Campastrino, Fig. 1) for detailed thin section petrographic analysis. From these, a representative set of sixty-five fresh and slightly altered samples was investigated for whole-rock geochemistry [4], while only very fresh igneous rocks (fifty-nine samples) was analysed (and data reported here) for petrography and mineral-glass chemical composition.

2.2. Optical microscopy

Thin section analyses for the modal mineralogy and petrography were performed using a polarizing light optical microscope Nikon Optiphot2-Pol, equipped with AxioScope Digital Camera.

2.3. Scanning electron microscopy (SEM)

In order to verify the semi-quantitative elemental composition and to be sure of acquiring data on unaltered samples, the APF rocks were examined by an Environmental Scanning Electron Microscope (ESEM) FEI Quanta 200 FEG, equipped with an energy-dispersive X-ray spectrometer (EDS) for micro-chemical analyses, at the University of Urbino Carlo Bo, Italy. Operating conditions were 30 kV accelerating voltage, 10 mm working distance, 0° tilt angle, and variable beam diameter. The ESEM was utilized in low vacuum mode, with a specimen chamber pressure set from 0.8 to 0.9 mbar. The electron beam was defocused, which is associated with a shortened accumulation time (from 100 s down to 10 s) and minimizes volatile migration and loss. The standards used were natural minerals and synthetic phases.

2.4. Electron microprobe (EMP)

After polishing and metallization, sixty-five thin sections were analyzed for mineral and glass chemical composition with a Cameca SX50 electron microprobe at the University of Rome La Sapienza (IGAG laboratory, CNR) and a Cameca Camebax 799 electron microprobe at the Istituto di Geoscienze e Georisorse, CNR, Padua, Italy. The operating conditions are 15 kV and 15 nA using full WDS, with a beam size ranging from $\sim 2\,\mu$m (for opaque minerals) to $\sim 5\,\mu$m (for feldspars, pyroxenes, amphibole and biotite) and $\sim 10\,\mu$m for glass analyses. Errors are $\pm 2\%$ for major and $\pm 5\%$ for minor elements. Standards comprise a series of pure elements, simple oxides or simple silicate compositions.

Recalculations of EMP chemical data were performed as follow: for pyroxenes, structural formulae, classification parameters and end-member components were calculated using the software PYROX [11] following the IMA rules [12]; for amphiboles, structural formulae and classification were calculated using the software NEWAMPHCAL [13] following the IMA rules [14]; for micas, structural formulae and classification were calculated using the software MICA+ [15]; for Fe-Ti oxides, structural formulae and ilmenite molecular fractions were calculated using the software ILMAT [16].

Declaration of Competing Interest

The authors declare that they have no known competing financial interests or personal relationships, which have, or could be perceived to have, influenced the work reported in this article.

Acknowledgments

MM gratefully acknowledge G. Zanzucchi (Parma, Italy) who encouraged discussions about Canetolo Unit and supporting fieldwork on the Northern Apennines realm. We wish to thank M. Serracino (Rome, CNR-IGAG) and R. Carampin (Padua, Italy, CNR-IGG) for their skilled assistance during electron microprobe analyses. Very constructive suggestions and comments by an anonymous reviewer significantly improved the manuscript. ML and SR acknowledges Fondi Ateneo Sapienza 2018 and 2019.

Supplementary materials

Supplementary material associated with this article can be found, in the online version, at doi:10.1016/j.dib.2020.106015.

References

[1] P. Elter, R. Catanzariti, F. Ghiselli, M. Marroni, G. Molli, G. Ottria, L. Pandolfi, L'Unità Aveto, (Appennino settentrionale); caratteristiche litostratigrafiche, biostratigrafia, petrografia delle areniti ed assetto strutturale, Boll. Soc. Geol. Ital. 118 (1999) 41–63.

[2] M. Mattioli, G. Di Battistini, G. Zanzucchi, Petrology, geochemistry and age of the volcanic clasts from the Canetolo Unit (Northern Apennines, Italy), Boll. Soc. Geol. Ital. Vol. Spec. 1 (2002) 399–416.

[3] M. Mattioli, G. Di Battistini, G. Zanzucchi, Geochemical features of the Tertiary buried Mortara volcanic body (Northern Apennines, Italy), Boll. Soc. Geol. Ital. Vol. Spec. 1 (2002) 239–249.

[4] M. Mattioli, M. Lustrino, S. Ronca, G. Bianchini, Alpine subduction imprint in Apennine volcaniclastic rocks. Geochemical-petrographic constraints and geodynamic implications from Early Oligocene Aveto-Petrignacola Formation (N Italy), Lithos 134 (2012) 201–220, doi:10.1016/j.lithos.2011.12.017.

[5] L. Beccaluva, G. Bianchini, M. Coltorti, F. Siena, M. Verde, 2005. Cenozoic tectono-magmatic evolution of the central-western Mediterranean: migration of an arc-interarc basin system and variations in the mode of subduction, in: I. Finetti (Ed.), Crop Project - Deep Seismic Exploration of the Central Mediterranean and Italy, Elsevier, 2005, pp. 623–640. Special Volume.

[6] C.L. Rosenberg, Shear zones and magma ascent: a model based on a review of the tertiary magmatism in the Alps, Tectonics 23 (2004) TC3002, doi:10.1029/2003TC001526.

[7] O.A. Anfinson, M.G. Malusà, G. Ottria L.N. Dafov, D.F. Stockli, Tracking coarse-grained gravity flows by LASS-ICP-MS depth-profiling of detrital zircon (Aveto Formation, Adriatic foredeep, Italy), Marine Petrol. Geol. 77 (2016) 1163–1176, doi:10.1016/j.marpetgeo.2016.07.014.

[8] A. Di Capua, L. Vezzoli, G. Groppelli, Climatic, tectonic and volcanic controls of sediment supply to an Oligocene foredeep basin: the val d'Aveto Formation (Northern Italian Apennines), Sediment. Geol. 332 (2016) 68–84, doi:10.1016/j.sedgeo.2015.11.009.

[9] M. Mattioli, A. Renzulli, B.G.J. Upton, Sub-volcanic crystallization at Sete Cidades, Sao Miguel, Azores as inferred from mafic and ultramafic plutonic nodules, Mineral. Petrol. 60 (1997) 1–26.

[10] M. Mattioli, G. Serri, E. Salvioli-Mariani, A. Renzulli, P.M. Holm, P. Santi, G. Venturelli, Sub-volcanic infiltration and syn-eruptive quenching of liquids in cumulate wall-rocks: the example of the gabbroic nodules of Stromboli (Aeolian Islands, Italy), Mineral. Petrol. 78 (2003) 201–230.

[11] F. Yavuz, PYROX: a computer program for the IMA pyroxene classification and calculation scheme, Comput. Geosci. 27 (2001) 97–107.

[12] N. Morimoto, J. Fabries, A.K. Ferguson, I.V. Ginzburg, M. Ross, F.A. Seifert, J. Zussman, K. Aoki, D. Gottardi, Nomenclature of pyroxenes, Am. Mineral. 62 (1988) 53–62.

[13] F. Yavuz, A revised program for microprobe-derived amphibole analyses using the IMA rules, Comput. Geosci. 25 (1999) 909–927.

[14] B.E. Leake, A.R. Woolet, C.E.S. Arps, W.D. Birch, M.C. Gilbert, J.D. Grice, F.C. Hawthorne, A. Kato, H.J. Kisch, Krivovichev, et al., Nomenclature of amphiboles: report of the subcommittee on amphiboles of the international mineralogical association, commission on new minerals and mineral names, Can. Mineral. 35 (1997) 219–246.

[15] F. Yavuz, Evaluating micas in petrologic and metallogenic aspect: I-definitions and structure of the computer program MICA+, Comput. Geosci. 29 (2003) 1203–1213.

[16] L.D. Lepage, ILMAT: an excel worksheet for ilmenite-magnetite geothermometry and geobarometry, Comput. Geosci. 29 (2003) 673–678.

[17] T.N. Irvine, W.R.A. Baragar, A guide to chemical classification of common volcanic rocks, Can. J. Earth Sci. 8 (1971) 523–548.